Optimization of Cyclone Geometry for Bauxite Beneficiation

Allan Suhett Reis[1], Geraldo Magela Pereira Duarte[2], Eslyn Neves[3], Thiago Jatobá and José Erik Araujo[5]
1. R&D Consultant
2. Senior R&D Specialist
3. Process and Laboratory Manager
Hydro Bauxite & Alumina, Paragominas, Brazil
4. Partner
MinPro Solutions, São Paulo, Brazil
5. Senior R&D Manager
Hydro Bauxite & Alumina, Barcarena, Brazil
Corresponding author: allan.reis@hydro.com
https://doi.org/10.71659/icsoba2024-bx007

Abstract

Bauxite is the main ore for alumina and then primary aluminium production, consisting mainly of gibbsite, as aluminium source, iron oxides such as goethite and hematite and kaolinite, a clay mineral commonly found in Amazonian bauxites, as the main carrier of reactive silica. In the process, due to the small particle size, kaolinite is usually removed by attrition and washing of coarse material followed by desliming using hydrocyclones. Kaolinite has a special relevance in this context as in the Bayer process, it reacts with sodium hydroxide, thus increasing caustic consumption in the process. Beneficiation process at Hydro Paragominas is based on the separation of coarser fractions with higher gibbsite content from the clay minerals, where kaolinite is more concentrated. The separation takes place in two-stage hydrocyclone circuits, one for mid-size particles classification and another for fine particles classification. Pilot tests and process simulations have been carried out seeking the optimization of cyclone geometry, by testing different apex and vortex diameters. A total of 36 different conditions were evaluated with optimized condition bringing reactive silica reduction potential of 1.3 percentual points.

Keywords: Bauxite beneficiation, Clay removal, Silica reduction, Hydrocyclones.

1. Introduction

Bauxite is a rock composed by aluminium oxides/hydroxides and is the main ore for production of primary aluminium. Amazonian bauxite, processed by Hydro Paragominas, are mostly composed of gibbsite as the main mineral and gangue composed of kaolinite, iron oxides (hematite and goethite), titanium oxides (rutile and anatase) and quartz [1–5].

Kaolinite, the source mineral for reactive silica, is a clay mineral and due to its fine particle size is usually removed from the process in desliming steps using hydro-cyclones. A special attention is paid to kaolinite in this context as in the Bayer process, it reacts with sodium hydroxide, increasing the caustic consumption in the process by forming desilication products [6–8].

Available alumina concentration and reactive silica removal on bauxite beneficiation through desliming in hydrocyclone steps is based on the chemical profile, shown in Figure 1. The combination of the high costs associated to processing kaolinite at the refinery and bauxite chemical composition on different particle sizes, with high reactive silica and low available alumina grades on the fraction finer than 10 μm is the main motivation to develop the present work, seeking optimized apex and vortex finder diameters to maximize reactive silica removal on Hydro Paragominas beneficiation plant.

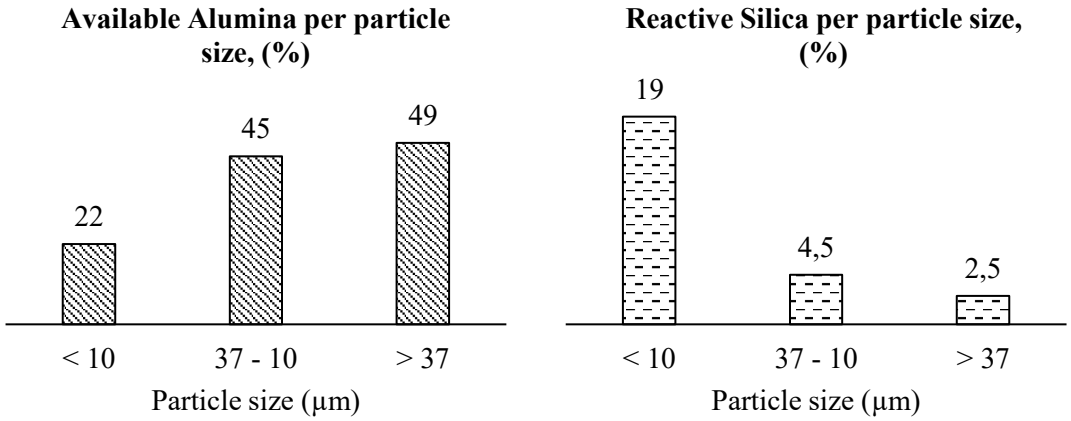

Figure 1. Amazonian bauxite chemical profile on different particle sizes [6]

2. Materials and Methods

2.1 Hydro Paragominas' Beneficiation Plant

Hydro Paragominas' bauxite processing circuit includes three main classification steps to separate the coarser fraction, with higher gibbsite content, from the finer fraction, where most of the kaolinite is concentrated. The first step is also responsible for separating fine particles from pebbles, which is followed by the re-crushing process, and is carried out on vibrating screens. The second step, called mid-size particles classification circuit, is carried out in 660 mm diameter hydrocyclones and separates clay and finer bauxite particles, from mid-size particles, that feeds the ball mill. The third step, called fine particles classification circuit, is carried out in 254 mm diameter hydrocyclones and is the final step for separation of clay, beneficiation process tailings, to fine bauxite particles, that forms the product. A simplified flowchart of the processing plant is presented in Figure 2.

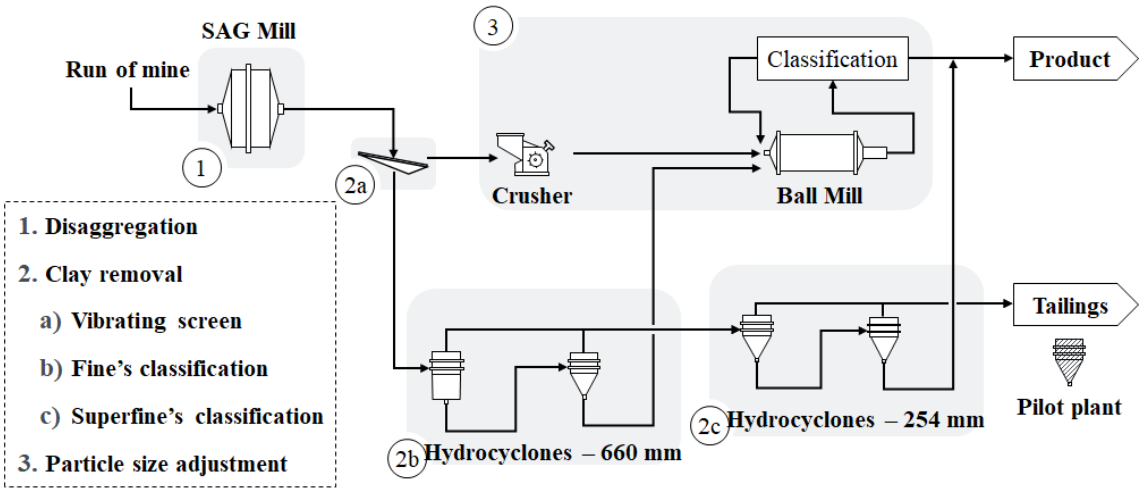

Figure 2. Hydro Paragominas' beneficiation plant simplified flowchart.

2.2 Pilot Equipment

A pilot plant was installed at the beneficiation plant to support process evaluations on fines classification circuit. The equipment has been used on pilot tests to evaluate the performance on

both primary and secondary steps of classification. Main design and operational specifications from the pilot plant are listed below:

- 1 hydrocyclone with 254 mm diameter (same from industrial superfines circuit)
- Flow rate: 85–150 m³/h
- Operating pressure: 245–314 kPa
- Operation in batches, with a 3 m³ slurry tank, with agitator

Pilot tests were carried out by filling the slurry tank with bauxite slurry from the industrial plant cyclones feed. The slurry pump was used to feed the hydrocyclone. Both underflow and overflow were recirculated to the feed tank, forming a closed circuit. Sampling devices on the three cyclone flows were used to get bauxite samples for laboratory analysis, as shown in Figure 3.

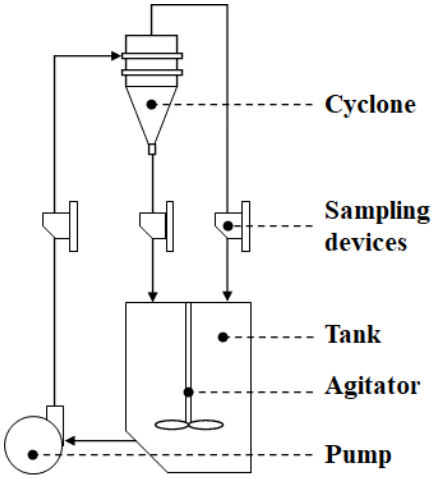

Figure 3. Pilot plant schematic flows.

2.3 Material and Characterization Methods

Bauxite used on pilot tests were from Hydro Paragominas beneficiation plant. Two testing campaigns were carried out, one processing the primary step of classification feed and the other processing the secondary step of classification feed.

Sampling points were located near to industrial plant cyclones feed, tanking the material on the slurry density that were feeding the cyclones. The slurry was then directed by gravity to the pilot plant tank.

On pilot tests, for each operating condition one sample was taken from each flow and was submitted to characterization as described below:

- The sample was dried in a laboratory stove at 105 ºC to determine the percentual of solids. Dry samples were quartered to generate aliquots for chemical and particle size analysis.
- PSD: Wet screening for particle size distribution analysis from 600 µm to 37 µm. The fraction finer than 37 µm was submitted to laser diffraction analysis (Malvern);
- X-Ray analysis: Samples were submitted to total oxides analysis (Al_2O_3, Fe_2O_3, SiO_2 and TiO_2) through X-Ray Fluorescence.
- Available alumina and reactive silica concentration analysis: Bauxite samples were dried at 105 °C, ground in planetary mill until 100% finer than 105 µm and submitted to digestion with caustic soda in PARR bombs for 25 minutes, at 150 °C. After digestion, the samples were submitted to slow filtration with #42 filter paper, generating two fractions:

- Liquor passing the filter paper: The liquor was prepared to the determination of available alumina grade using titration. The samples received hydrochloric acid, methyl red indicator, complexing agent CDTA, hexamethylenetetramine buffer solution, orange xylene indicator and were then submitted to titration with zinc sulphate solution on Oil Titrando 905 equipment.
- Solids retained on filter paper: The solid material from the filtration process were submitted to acid digestion with hydrochloric acid for further reactive silica analysis on Agilent 240 FS Atomic Absorption spectrometer.

2.4 Testing Plan

The work had as objective to define the optimized operating condition for the fines circuit at Hydro Paragominas beneficiation plant in terms of removing clay minerals / reactive silica. Different apex and vortex diameters were tested on both primary and secondary steps of classification, as shown in Table 1.

Table 1. Bauxite chemical composition.

Testing condition	1	2	3	4	5	6
Vortex diameter (mm)	102	102	102	89	89	89
Apex diameter (mm)	51	44	38	51	44	38
Apex / Vortex ratio	0.50	0.43	0.37	0.57	0.49	0.43

Testes were carried out in two batches; one reproducing the primary and the other reproducing the secondary step of classification, with the 6 conditions presented in Table 1 tested in each batch.
Test results were analysed and used to fit the calibration constants from Nageswararao[9] model for hydrocyclones. With the model calibrated for each of the two classification steps, a simulation model was developed to evaluate performance on the fines circuit, with primary step underflow feeding secondary step, after slurry density control with water dilution. A total of 36 simulation scenarios were developed, combining each different condition tested. Main outcomes from the simulation were mass / metallurgical recoveries, av. alumina and re. silica grades and particle size distribution for each process flows on the fines circuit individually and integrated with the plant, to estimate the benefits and potential impacts over the full beneficiation process.

3. Results and Discussion

3.1 Bauxite Characterization

Table 2 shows each classification step feed chemical characterization, with higher available alumina grade and lower reactive silica grade on secondary step feed. The results are consistent with typical Amazonian bauxite granulochemical profile, wherein finer particles, below 10 µm has higher concentration of gangue minerals and thus, lower alumina and higher silica grades.

Table 2. Classification steps feed chemical characterization.

Classification Step	Av. Alumina (%)	Re. Silica (%)
Primary	24.59	18.48
Secondary	36.70	10.12

Figure 4 shows the particle-size distribution of the pilot tests feed. Primary step presents a high concentration of slimes, with 58% of the particles finer than 10 µm. Secondary step feed presets a significatively lower concentration of slimes, with 31 % of the particles finer than 10 µm. The

difference between the curves is associated to the fact that secondary step feed is the underflow from the primary step of desliming on the fines circuit.

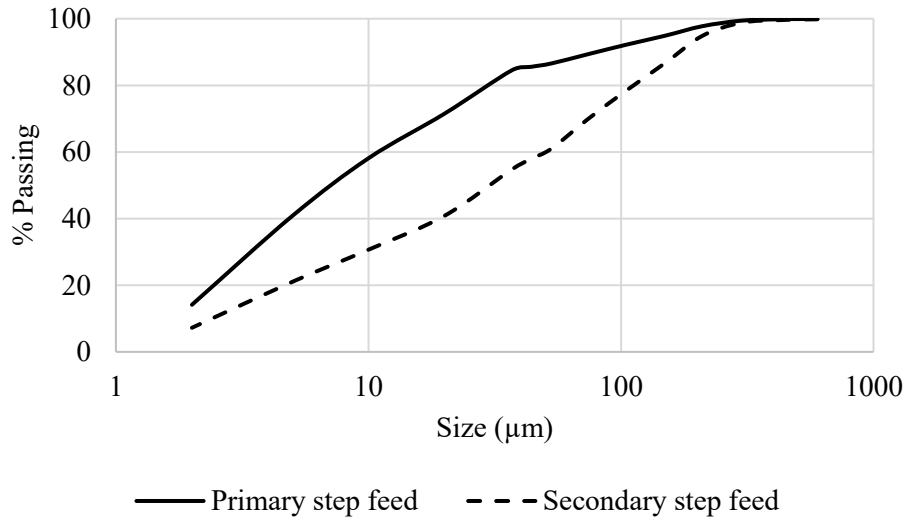

Figure 4. Particle size distribution for pilot tests feed.

Full pilot tests flows characterization is presented on tables 3 to 6.

Table 3. Pilot tests flows characterization – Primary step (1/2).

Flow	Feed	Under	Over	Feed	Under	Over	Feed	Under	Over
Apex (mm)	38	38	38	44	44	44	51	51	51
Vortex (mm)	102	102	102	102	102	102	102	102	102
% < 600 µm	100.0	99.8	100.0	100.0	99.8	100.0	100.0	99.7	100.0
% < 150 µm	94.9	76.9	100.0	94.7	78.9	100.0	95.1	81.4	100.0
% < 74 µm	89.4	52.4	99.9	89.2	56.8	99.9	89.7	62.2	99.9
% < 44 µm	86.0	35.8	99.8	85.5	41.1	99.8	85.8	49.8	99.8
% < 20 µm	67.6	19.1	84.1	71.3	25.1	86.1	72.6	32.8	87.8
% < 10 µm	52.6	13.9	64.8	56.2	18.2	69.3	58.9	24.5	71.4
% solids	10.2	42.9	8.8	10.8	34.0	8.8	10.9	26.6	8.7
% Av. Alumina	24.4	43.0	18.8	24.7	41.2	18.7	24.6	38.6	18.6
% Re. Silica	18.9	7.3	23.1	18.6	8.0	23.1	18.9	9.0	23.1
% Total Al_2O_3	43.4	50.1	41.3	43.1	49.1	41.2	43.3	48.6	41.0
% Fe_2O_3	12.3	11.5	12.8	12.3	11.6	12.6	12.3	11.2	12.8
% Total SiO_2	19.7	7.9	23.7	19.4	8.9	23.5	19.5	10.2	23.9
% TiO_2	2.1	3.2	1.8	2.1	3.1	1.8	2.1	2.8	1.9
% LOI	21.4	26.3	19.8	21.4	25.7	19.8	21.3	25.2	19.7

Table 4. Pilot tests flows characterization – Primary step (2/2).

Flow	Feed	Under	Over	Feed	Under	Over	Feed	Under	Over
Apex (mm)	38	38	38	44	44	44	51	51	51
Vortex (mm)	89	89	89	89	89	89	89	89	89
% < 600 µm	99.9	99.7	100.0	99.9	99.7	100.0	99.9	99.8	100.0
% < 150 µm	95.0	81.2	99.9	94.9	83.3	100.0	94.9	85.1	99.9
% < 74 µm	89.2	61.6	99.7	89.4	65.8	99.9	89.2	70.9	99.8
% < 44 µm	85.1	48.6	99.5	85.8	53.9	99.8	85.3	61.2	99.8
% < 10 µm	58.6	22.8	74.7	62.1	27.3	74.1	60.4	34.5	73.2
% solids	10.9	29.1	8.5	10.9	25.5	8.4	10.9	27.5	8.4
% Av. Alumina	24.8	38.9	18.5	24.7	37.8	18.3	24.7	35.5	18.1
% Re. Silica	18.4	7.9	21.8	18.4	10.3	23.2	18.4	10.9	22.0
% Total Al_2O_3	43.2	48.8	41.4	43.3	48.2	41.0	43.3	47.3	40.9
% Fe_2O_3	12.2	11.3	12.2	11.9	11.6	12.6	11.8	11.5	12.1
% Total SiO_2	19.4	10.0	23.0	19.0	10.9	23.9	18.7	12.3	23.0
% TiO_2	2.1	2.8	1.8	2.1	2.8	1.8	2.0	2.5	1.7
% LOI	21.3	25.2	19.6	21.4	25.0	19.5	21.4	24.3	19.5

Table 5. Pilot tests flows characterization – Primary step (1/2).

Flow	Feed	Under	Over	Feed	Under	Over	Feed	Under	Over
Apex (mm)	38	38	38	44	44	44	51	51	51
Vortex (mm)	102	102	102	102	102	102	102	102	102
% < 600 µm	99.8	99.7	100.0	99.8	99.6	100.0	99.8	99.7	100.0
% < 150 µm	86.7	76.5	99.9	86.6	78.3	99.9	87.6	79.3	100.0
% < 74 µm	70.6	46.7	99.9	70.3	48.7	99.9	70.7	50.6	99.9
% < 44 µm	59.4	26.1	99.7	58.4	28.7	99.7	59.0	30.9	99.8
% < 10 µm	29.4	3.9	60.2	29.7	4.3	58.3	32.9	6.5	57.2
% solids	13.1	67.8	6.5	13.2	66.8	6.3	13.2	54.7	6.0
% Av. Alumina	36.6	46.4	24.3	36.5	46.1	23.8	36.9	45.2	23.4
% Re. Silica	10.6	4.6	18.7	10.9	3.9	19.2	10.1	5.1	18.8
% Total Al_2O_3	47.2	50.7	42.7	47.3	50.9	42.5	47.4	50.4	42.5
% Fe_2O_3	13.4	12.4	14.8	13.5	12.6	14.8	13.5	12.8	14.6
% Total SiO_2	11.2	5.0	19.3	11.4	5.2	19.7	11.2	5.8	20.0
% TiO_2	2.9	3.5	2.1	2.9	3.4	2.1	2.9	3.3	2.1
% LOI	24.4	27.0	21.0	24.3	27.0	21.0	24.4	26.8	20.9

Table 6. Pilot tests flows characterization – Primary step (2/2).

Flow	Feed	Under	Over	Feed	Under	Over	Feed	Under	Over
Apex (mm)	38	38	38	44	44	44	51	51	51
Vortex (mm)	89	89	89	89	89	89	89	89	89
% < 600 µm	99.8	99.6	100.0	99.8	99.7	100.0	99.8	99.7	100.0
% < 150 µm	85.3	77.6	99.9	87.2	77.1	99.9	85.5	81.3	100.0
% < 74 µm	68.0	49.0	99.8	69.1	50.2	99.9	68.4	55.3	99.9
% < 44 µm	55.9	29.6	99.7	57.1	31.8	99.8	55.7	45.5	99.8
% < 10 µm	29.1	6.0	63.9	30.6	6.1	60.8	30.1	13.5	63.5
% solids	13.5	65.2	5.5	14.8	56.2	5.5	14.1	39.5	5.5
% Av. Alumina	36.8	44.2	23.1	36.6	44.3	22.7	36.8	43.4	22.2
% Re. Silica	10.1	5.9	20.0	10.5	5.1	19.5	10.1	6.3	20.0
% Total Al_2O_3	47.2	49.7	42.3	47.3	50.1	42.1	47.2	49.8	41.9
% Fe_2O_3	13.4	13.0	14.4	13.5	12.9	14.4	13.5	13.0	14.6
% Total SiO_2	11.1	6.2	20.3	11.3	6.2	20.4	11.2	6.8	20.6
% TiO_2	2.8	3.3	2.1	2.9	3.3	2.1	2.9	3.2	2.1
% LOI	24.4	26.4	20.8	24.4	26.5	20.6	24.4	26.3	20.5

3.2 Pilot Tests

Pilot test results were evaluated in terms of available alumina recovery to underflow and reactive silica removal to overflow (tailings) on each classification step and testing condition. Figure 5 shows the results for the primary step of classification. Two main patterns were observed on testing results, higher silica removal in conditions 1, 2 and 3, with larger vortex finder diameter when compared to conditions 4, 5 and 6; and when comparing results with the same vortex finder diameters, higher silica removal potentials were found with smaller apex diameters.

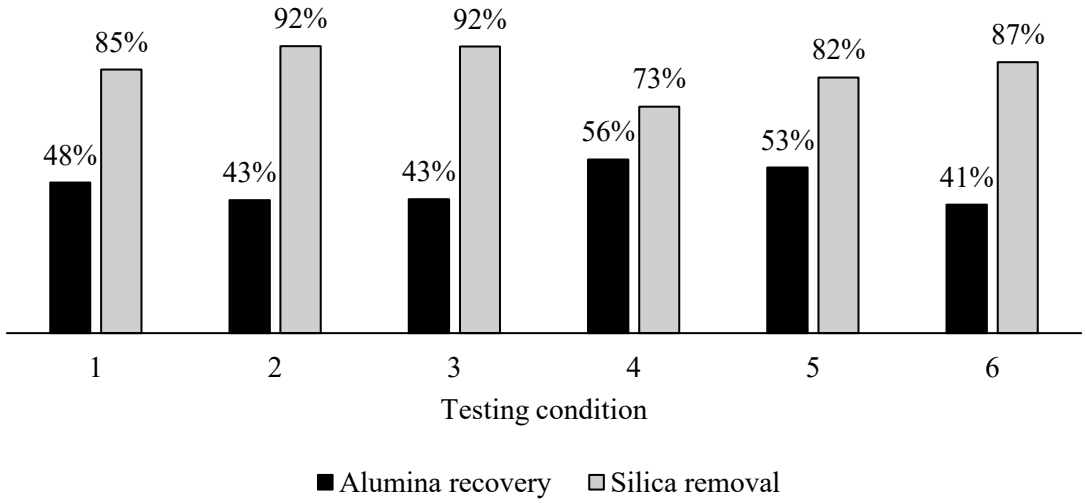

Figure 5. Available alumina recovery to underflow and reactive silica removal to overflow on different testing conditions for primary step of classification tests.

Figure 6 shows the results for the secondary step of classification. The same patterns observed for the primary step of classification were found on tests with the secondary step. Another outcome from the tests with the secondary step is that higher alumina recoveries and lower silica removals were obtained on those tests, when compared to the ones with the primary step. This behaviour is mainly associated to the lower concentration of low-grade fine particles on secondary step feed, bring lower removal of silica, and also lower losses of alumina, as the fine particles carries some alumina content.

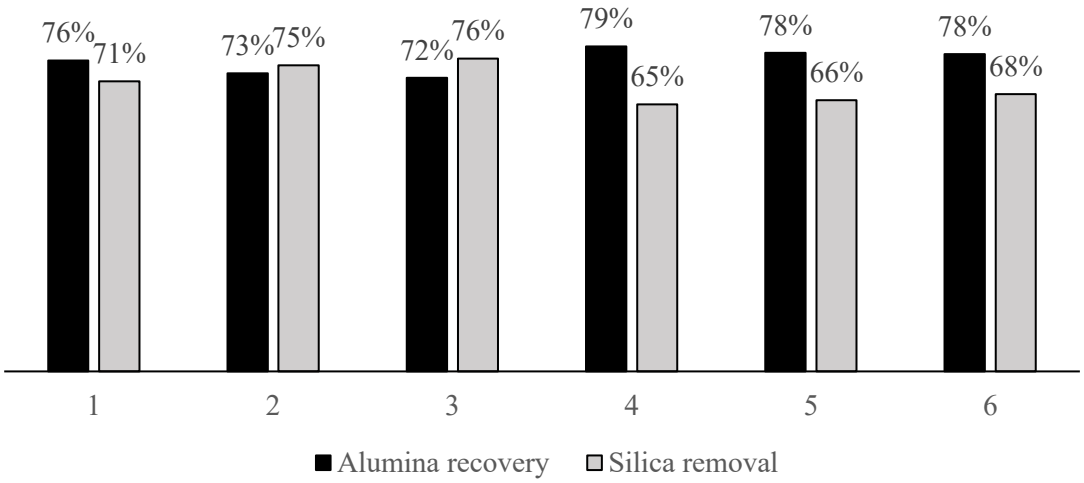

Figure 6. Available alumina recovery to underflow and reactive silica removal to overflow on different testing conditions for secondary step of classification tests.

Another outcome from the tests is associated to the relation between the desliming performance, measured by the indicators available alumina recovery to underflow and reactive silica removal to overflow, with apex / vortex diameter ratios. As shown in Figure 7, there is a tendency to get higher alumina recoveries and lower silica removal as apex / vortex ratio increases.

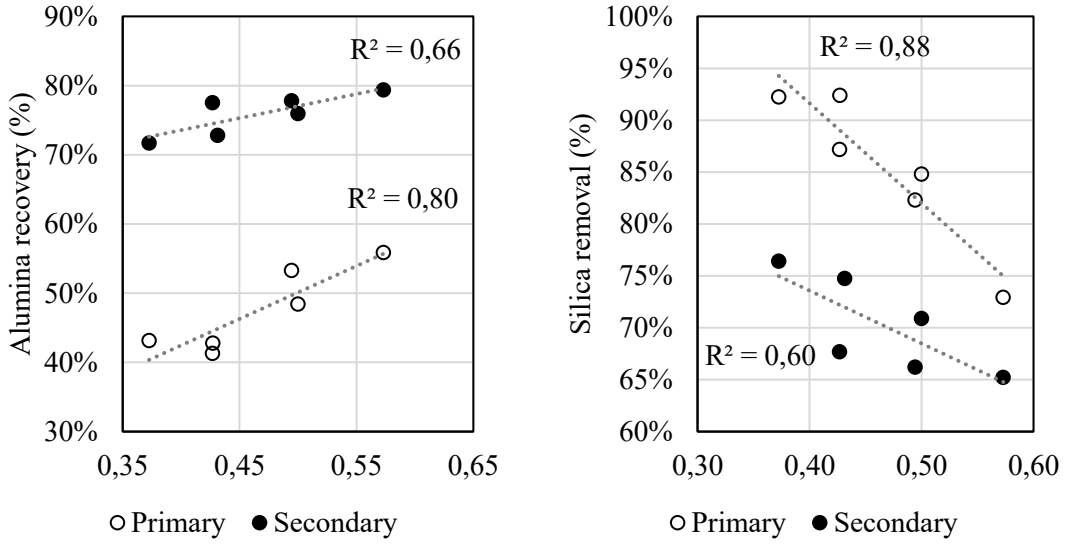

Figure 7. Available alumina recovery to underflow (left) and reactive silica removal to overflow (right) for different apex / vortex diameter ratios on primary and secondary steps.

3.3 Process simulation

Process simulations combining the different scenarios tested in pilot scale allowed finding the optimized condition in terms of reactive silica removal on the beneficiation plant and the quantification of the associated impacts on available alumina recovery. The results from 36 simulated scenarios are shown in Figure 8, where the results from current plant setup are highlighted in a blue triangle (primary step using 89 mm vortex and 51 mm apex – Condition 4, and secondary step using 89 mm vortex and 44 mm apex – Condition 5).

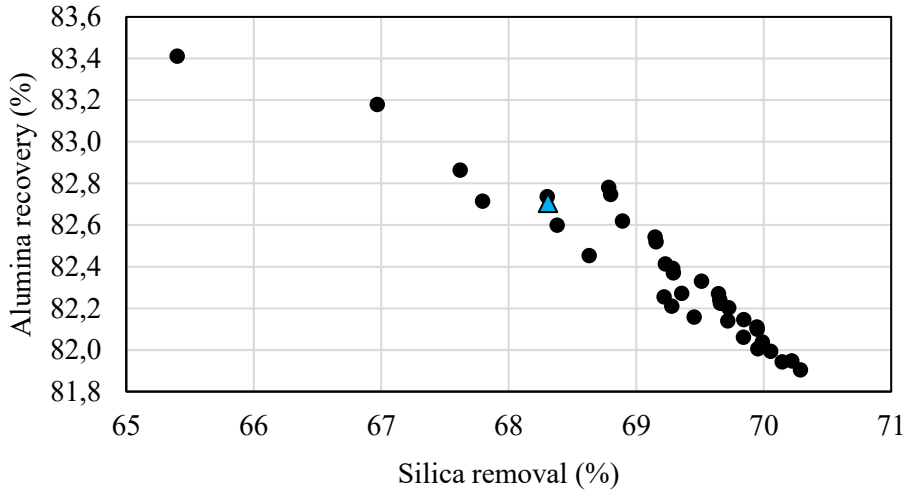

Figure 8. Simulated available alumina recoveries to product and reactive silica removal to tailings on Hydro Paragominas beneficiation plant.

A summary of base case scenario, with the beneficiation plant as it currently operates and estimated results with cyclone geometry optimization is show in table 7.

Table 7. Summary of key process indications with and without cyclone geometry optimization.

Indicator	Plant as it is	Plant with cyclone optimization	Variation
Plant product av. alumina grade (%)	47.57	47.96	0.40
Plant product re. silica grade (%)	4.80	4.61	0.19
Alumina recovery on beneficiation (%)	82.71	81.90	0.79

Taking current plant performance as the base case scenario, it was possible to estimate the benefits and impacts from fines circuit optimization. In terms of product chemical quality, base case reactive silica grade for fines circuit underflow and beneficiation plant product are respectively 5.68 % and 4.80 %. Among the simulation scenarios, the best results obtained for reactive silica removal were found with 102 mm vortex and 38 mm apex on both primary and secondary steps, the lower apex / vortex diameter ratios evaluated for each step. For this scenario, simulated reactive silica for fines circuit underflow and beneficiation plant product were respectively 4.42 %

and 4.61 %, representing a 1.26 percentual points silica reduction on the fines circuit and a 0.19 percentual point reduction on beneficiation plant product silica grade. This higher silica reduction was associated to a reduction on alumina recovery at the beneficiation plant of 0.8 percentual points, from 82.7 % to 81.9 %.

At the refinery, processing the bauxite with 0.19 percentual points lower reactive silica grade would lead to a reduction on 1.4 kg of caustic per tonne of bauxite.

4. Conclusions

On both primary and secondary steps of classification, higher reactive silica reduction results were found for testing conditions with lower apex / vortex diameter ratio. On the conditions with higher silica reduction, higher alumina losses were observed, due to the presence, even in low concentration, of available alumina on the fine particles below 10 μm removed on the desliming process.

Among the 36 simulated scenarios, reactive silica reductions up to 1.26 percentual points on the fines circuit and 0.19 percentual points on the beneficiation plant product were found through:

- Replacing 89 mm diameter vortex by 102 mm ones on both classification steps;
- Replacing 51 mm diameter apex on primary step by 38 mm;
- Replacing 44 mm diameter apex on secondary step by 38 mm.

Higher silica reduction was associated to a reduction on alumina recovery at the beneficiation plant of 0.8 percentual points, from 82.7 % to 81.9 %.

5. References

1. Adão B. Luz, João A. Sampaio, Silvia C. França, Tratamento de Minérios, 5th Edition, Rio de Janeiro, CETEM/MCT, 2010. 932 pages.
2. Duarte et al. Reactive silica reduction on bauxite by flotation. *TRAVAUX* 52, *Proceedings of the 41st International ICSOBA Conference*, Dubai, 5 - 9 November 2023, pages 303 – 305
3. F. M. MEYER, Availability of Bauxite Reserves. *Natural Resources Research*, Volume 13, pages 161 - 172, September 2004, *Springer Science and Business Media LLC*.
4. Marcondes L. Costa et al., On the geology, mineralogy and geochemistry of the bauxite-bearing regolith in the lower Amazon basin: Evidence of genetic relationships, *Journal of Geochemical Exploration*, Volume 146, pages 58 - 74, November 2014, *ELSEVIER BV*.
5. Otávia M. Rodrigues et al., Kaolinite and hematite flotation separation using etheramine and ammonium quaternary salts. Minerals Engineering, Volume 40, pages 12 - 15, January 2013, ELSEVIER BV.
6. Reis et al. Pilot tests with tertiary cyclone for reactive silica removal from Amazonian Bauxite. *TRAVAUX* 52, *Proceedings of the 41st International ICSOBA Conferenc*e, Dubai, 5 - 9 November 2023, pages 293 - 302.
7. José F. Gomes et al., The formation of desilication products in the presence of kaolinite and halloysite – The role of surface area, Hydrometallurgy, Volume 203, article 105643, August 2021, ELSEVIER BV.
8. Peter Smith, The processing of high silica bauxites – Review of existing and potential processes. Hydrometallurgy, Volume 98, pages 162 - 176, August 2009, ELSEVIER BV.
9. Nageswararao, K. A generalised model for hydrocyclone classifiers. AusIMM Proceedings, Parkville, December 1995. v. 2, n. 300, 21 p